HHS Public Access

Author manuscript

J Comp Neurol. Author manuscript; available in PMC 2020 November 01.

Published in final edited form as:

J Comp Neurol. 2019 November 01; 527(16): 2730–2741. doi:10.1002/cne.24704.

Ultrastructural localization of cannabinoid-1 (CB1) and mGluR5 receptors in the prefrontal cortex and amygdala

Megan L. Fitzgerald[1,*], **Ken Mackie**[2], **Virginia M. Pickel**[1]

[1]Weill Cornell Medicine, Feil Family Brain and Mind Research Institute, 407 East 61st Street, New York, NY 10065 Fax: (646)962-0535

[2]Department of Psychological and Brain Sciences, Indiana University, 1101 E 10th St, Bloomington, IN 47405

Abstract

Stimulation of the postsynaptic metabotropic glutamate receptor mGluR5 triggers retrograde signaling of endocannabinoids that activate presynaptic cannabinoid CB1 receptors on juxtaposing axon terminals. To better understand the synaptic structure that supports mGluR5 mediation of CB1 activation in the prefrontal cortex (PFC) and basolateral amygdala (BLA), we examined electron microscopic dual immunolabeling of these receptors in the prelimbic PFC (prPFC) and BLA of adult male rats. CB1 immunoreactivity was detected in axon terminals that were typically large, complex, and contained dense-core and clear synaptic vesicles. Of terminals forming discernible synaptic specializations, 95% were symmetric inhibitory-type in the prPFC and 90% were inhibitory in the BLA. CB1-immunoreactive terminals frequently contacted dendrites containing mGluR5 adjacent to unlabeled terminals forming excitatory-type synapses. Because most CB1-containing terminals form inhibitory-type synapses, the unlabeled axon terminals forming asymmetric synapses are the likely source of the mGluR5 ligand glutamate. In the prPFC, serial section analysis revealed that GABAergic CB1-containing axon terminals targeted dendrites adjacent to glutamatergic axon terminals, often near dendritic bifurcations. These observations provide ultrastructural evidence that cortical CB1 receptors are strategically positioned for integration of synaptic signaling in response to stimulation of postsynaptic mGluR5 receptors and facilitation of heterosynaptic communication between multiple neurons.

Graphical Abstract

Corresponding author: Megan L. Fitzgerald, the Children's Hospital of Philadelphia, Department of Psychology, Abramson Research Center 515, 3615 Civic Center Boulevard, Philadelphia, PA 19104 Phone: (215)590-5670. Fax: (215)590-3709, fitzgeraml@email.chop.edu.

*Current affiliation: The Children's Hospital of Philadelphia, Department of Psychology, Abramson Research Center 515, 3615 Civic Center Boulevard, Philadelphia, PA 19104 Fax: (215)590-3709

Data Availability Statement:

The data that support the findings of this study are available from the corresponding author upon reasonable request.

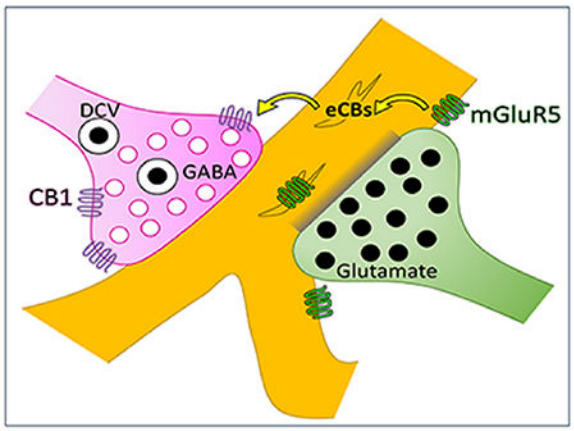

Cannabinoid CB1 receptors in the basolateral amygdala and prefrontal cortex of the rat brain are primarily located on inhibitory axon terminals, illustrated here in magenta. Presynaptic CB1 activation has been shown to attenuate GABA release. These GABAergic CB1 axon terminals often target dendrites (gold) that contain the metabotropic glutamate receptor mGluR5. The same dendrite is frequently also targeted by a different glutamatergic axon terminal (green). This ultrastructural architecture indicates the possibility of a mechanism of heterosynaptic plasticity where activation of mGluR5 receptors by glutamate released from one axon terminal can induce endocannabinoid signaling through CB1 receptors and thereby attenuate GABAergic vesicle release from a neighboring axon terminal.

Keywords

electron microscopy; endocannabinoids; glutamate; heterosynaptic plasticity; prelimbic

Introduction

The cannabinoid CB1 receptor is expressed in high levels in the prefrontal cortex (PFC), hippocampus, and amygdala-- brain regions critical to forming memories, processing emotions, and cognition (Herkenham et al. 1991). These functions are all dictated by the overarching molecular and cellular process of synaptic plasticity, and the CB1 receptor is a widespread mediator of activity-dependent changes in synaptic strength. The CB1 receptor mediates the effects of Δ9-tetrahydrocannabinol (THC), the primary psychoactive component of marijuana, in the central nervous system. Two endogenous ligands, both lipids, and termed endocannabinoids (eCBs), are known: anandamide and 2-arachidonoylglycerol (2-AG) (Devane et al. 1992; Stella et al. 1997).

To induce long-term and short-term changes in synaptic signaling, presynaptic CB1 receptors have been shown to act in concert with the postsynaptic metabotropic glutamate receptor mGluR5 (Wilson and Nicoll 2001). Effects on Group 1 mGluR mediated plasticity are blocked by CB1 receptor antagonists (Maejima et al. 2001), and mGluR5 is the Group 1 receptor subtype responsible for the induction of eCB signaling in the hippocampus and cortex (Varma et al. 2001; Lovinger 2008).

The proposed mechanism for this involves presynaptic release of glutamate, which binds postsynaptic mGluR5 receptors and induces release of endocannabinoids (eCBs) (Maejima *et al.* 2001; Wilson and Nicoll 2001). The eCBs then retrogradely activate Gi-coupled CB1 receptors located on the juxtaposing presynaptic terminal, resulting in suppression of synaptic vesicle release. CB1 receptor activation can induce inhibition of transmitter release from either GABAergic or glutamatergic axon terminals.

In many cortical regions, including the medial PFC, mGluR5-mediated CB1 receptor activation also induces suppression of excitatory signaling (Lafourcade et al. 2007). However, in the PFC, the somatosensory cortex, and the amygdala, the vast majority of synapses containing detectible CB1 form symmetric inhibitory-type junctions (Kotecha et al. 2003; Bodor et al. 2005; Hill, McLaughlin, et al. 2011). This raises the question of whether mGluR5 is more robustly positioned for participation in glutamatergic suppression of GABA release resulting from the activation of presynaptic CB1 receptors in GABAergic terminals in the PFC and basolateral amygdala (BLA). Electrophysiological evidence for this type of CB1-directed heterosynaptic plasticity exists in the hippocampus (Chevaleyre and Castillo 2003) and BLA (Zhu and Lovinger 2005). Furthermore, mGluR5 activation enhances excitatory PFC output through activation of presynaptic CB1 receptors (Kiritoshi et al. 2013), thereby implicating glutamate activation of mGluR5 in CB1-mediated suppression of GABAergic vesicle release in the PFC as well. However, anatomical evidence supporting this is lacking.

To test the hypothesis that the subcellular localization of CB1 and mGluR5 receptors is conducive to facilitation of heterosynaptic coordination in the PFC, dual immunoelectron microscopy was used to identify the relative pre- and post-synaptic locations of mGluR5 and CB1 receptors in the prelimbic region of the PFC (prPFC) and BLA of adult male rats. In the prPFC, GABA and glutamate are the major transmitters found in terminals that respectively form symmetric and asymmetric synapses. Thus, we used morphological criterion together with serial sectioning analysis of CB1-containing axon terminals to test the hypothesis that mGluR5 is positioned in a manner that could facilitate glutamate-induced endocannabinoid modulation of inhibitory transmission in the prPFC.

Materials and Methods

Animals

Group-housed male 3-month-old 325–350 gram Sprague-Dawley wild-type rats (N=3; RGD Cat# 10395233, RRID:RGD_10395233) were used in accordance with the NIH Institutional Guidelines for the Care and Use of Laboratory Animals and following a Research Animal Resource Center approved protocol. All efforts were made to minimize the number of animals used and their suffering. Animals were anesthetized with sodium pentobarbital (100 mg/kg, I.P. injection) prior to vascular perfusion via the ascending aortic arch with (1) 10 mL heparin-saline, (2) 60 mL 3.75% acrolein in 2% paraformaldehyde (PFA) in 0.1M phosphate buffer (PB; pH 7.4), and (3) 250mL 2% paraformaldehyde in PB. Brains were removed and fixed in 2% PFA at 4°C for 30 min prior to cutting coronal sections of fixed tissue at 40 μm thick on a Leica Vibratome. Sections through the BLA and PFC were

processed for immunohistochemistry (Fig 1a). The prPFC was sampled throughout all layers (Fig 1b), and the grid location of each micrograph was recorded.

Antibody characterization

CB1 was identified using an affinity-purified polyclonal antibody raised in guinea pig against a glutathione S-transferase fusion protein containing the C-terminus (residues 401–473) of rat CB1 (Berghuis et al. 2007) (Table 1). This antibody has been shown to have no immunoreactivity in CB1 knockout mice (Katona et al. 2006; Fitzgerald et al. 2012; Lane et al. 2012). mGluR5 was labeled with an affinity-purified synthetic rabbit polyclonal antibody raised against the C-terminus of mGlu5 (Chemicon AB5675; now Millipore-Sigma; RRID:AB_2295173). This antibody has been demonstrated to show no labeling in mGluR5 knockout tissue, labels a band of the correct molecular weight, and does not cross-react with mGluR1a (Kuwajima et al. 2004).

Immunohistochemistry

Immunohistochemical processing was conducted as previously described (Hill, McLaughlin, *et al.* 2011). Free-floating sections were first incubated in 1% sodium borohydride in 0.1M PB followed by successive washes of 0.1M PB. Tissue was then incubated in a cryoprotectant solution (25% sucrose, 3.5% glycerol in 0.05M PB) for 15 min, immersed in chlorodifluoromethane (Freon, Refron Inc., NY, USA), liquid nitrogen, and room temperature 0.1M PB. Tissue was then blocked in 0.5% bovine serum albumin (BSA; Sigma-Aldrich, St. Louis, MO) in Tris-buffered saline (TBS) for 30 min.

Coronal sections were incubated in an antibody cocktail containing guinea pig CB1 antisera at 1:2000 and rabbit mGluR5 antisera at 1:1000 in TBS pH 7.6 containing 0.1% BSA for 24 hours at room temperature followed by an overnight incubation at 4°C.

For immunoperoxidase labeling of the CB1 receptor, sections were rinsed numerous times in 0.1M TBS and incubated in 1:400 biotinylated donkey anti-guinea pig IgG (Jackson ImmunoResearch Laboratories) for 30 min. Sections were again rinsed multiple times in 0.1M TBS before incubation in avidin-biotin peroxidase complex (Vectastain Elite ABC Kit, Vector Laboratories) for 30 min, rinsing again, and placement in 0.022% 3,3'-diaminobenzidine with 0.0033% hydrogen peroxide in 0.1M TBS for 7 min.

Dual-labeling with immunogold-silver for mGluR5 directly followed. Sections of tissue were rinsed in 0.01M phosphate-buffered saline (PBS), blocked in 0.8% BSA with 0.1% gelatin for 10 min, and incubated in goat anti-rabbit IgG conjugated with ultrasmall colloidal gold (Electron Microscopy Sciences) for 2h. Sections were then washed, fixed in 2% glutaraldehyde for 10 min, and rinsed in 0.2M citrate buffer. Gold particles were then silver-enhanced using the IntenSE M kit (GE Healthcare) for 6 min. Tissue was rinsed in 0.1M PB and laid flat for post-fixation for 60 min in 2% osmium tetroxide. Following post-fixation, sections were rinsed in 0.1M PB and dehydrated using solutions containing increasing ethanol concentrations followed by propylene oxide. Post-fixed, dehydrated sections were incubated overnight in 1:1 propylene oxide and EPON epoxy resin (Electron Microscopy Sciences). The following day, sections were transferred to 100% EPON for 2h, flat-

embedded in EPON between two sheets of Aclar plastic, and dried in an oven under weights for 72 hours.

Electron microscopy

Flat-embedded tissue sections were cut into trapezoids, glued to EPON blocks with superglue and trimmed with a glass knife. The prPFC (all layers) and the BLA were excised for ultrastructural examination (Fig 1a, b). 70 nm ultra-thin sections were cut on a Leica EM UC6 Ultramicrotome using an Ultra45 diamond knife (Diatome), collected on copper mesh grids, and counterstained by floating the grids on 5% uranyl acetate (20 min), quickly rinsing in deionized (DI) water, submerging in Reynolds lead citrate (6 min), rinsing again in DI water, and drying on filter paper. Images were collected using a Philips CM10 transmission electron microscope (FEI) interfaced with an AMT Advantage HR/HR-B CCT Camera System (Advanced Microscopy Techniques) or a Tecnai transmission electron microscope (FEI). Images were acquired at the EPON-tissue interface at various magnifications (13500, 18500, 19000, 25000, 30000, and 34000) to best see postsynaptic specializations. The EPON-tissue interface is where the plastic embedding material contacts the immunolabeled tissue, representing the surface of the tissue. Immunogold penetration typically decreases with increasing tissue depth and thus consistently capturing images at the EPON-tissue interface is relevant to any comparisons of immunolabeling. For single-section analyses, images were captured wherever a CB1 immunoperoxidase-containing axon terminal was observed and mGluR5 immunogold labeling was also within the field of view to ensure examination of sections with penetration of both antibodies.

Profiles within the neuropil were classified according to the criteria set by Peters, Palay, and Webster (1991). Axon terminals had numerous synaptic vesicles and frequently formed synapses with dendrites, dendritic spines, or neuronal soma. Axonal processes were often bundled into groups and also typically contained synaptic vesicles. Dendritic profiles were typically oval or elongated in shape and did not contain synaptic vesicles, but often contained mitochondria and sometimes an abundance of smooth endoplasmic reticulum. Dendritic spines were mushroom or knob-shaped, did not contain mitochondria, and showed a thickened post-synaptic membrane specialization apposing vesicle-filled axon terminals. Glial profiles were irregularly shaped and often encased other structures within the neuropil. Cell somata were characterized by their large size, the presence of nuclei, large quantity of mitochondria, endoplasmic reticulum, Golgi, and other subcellular components. Neuronal somata were also targeted by many axon terminals. Profiles categorized as ‘unidentifiable’ were typically either partially occluded by a grid bar or were small and round and therefore it was difficult to distinguish definitively whether they were a small axon process or a spine neck cross-section. Symmetric synapses typical of GABAergic terminals were defined by thin post-synaptic specializations while asymmetric (glutamatergic) synapses had thick electron-dense post-synaptic specializations. mGluR5 immunogold labeling was punctate, approximately 40 nm in diameter, whereas CB1 immunoperoxidase labeling formed a diffuse reaction product that appeared as darker than similar profiles in the surrounding neuropil.

Analysis and presentation of mGluR5 immunogold labeling and single section electron micrographs

MCID Elite computer software version 6.0 (St. Catherines, ON, Canada) was used to determine the distance between mGluR5 immunogold particles and the synaptic specialization. The system was calibrated according to the magnification of the electron micrograph, and distances were measured in nm. The distance from the center of each immunogold particle to the nearest point on the synaptic specialization was measured and recorded from all images containing synaptic specializations presynaptic to mGluR5-containing dendritic profiles. Both cytoplasmic and plasmalemmal mGluR5 immunogold particles were included, because mGluR5 activation, internalization, and recycling back to the surface membrane is a dynamic and continuous process (Trivedi and Bhattacharyya 2012). Averages and standard deviations were calculated using Microsoft Excel (Microsoft Office Professional Plus 2016). An unpaired t-test was used to compare the average distance of mGluR5 immunogold particles from the symmetric synaptic specializations formed by CB1-containing axon terminals to the distance of mGluR5 immunogold to asymmetric synaptic specializations formed by unlabeled axon terminals. Significance was determined at $p < 0.05$. Electron micrographs were labeled and compiled for figure presentation using Adobe Photoshop CC (2015.0.0 release) and Microsoft Powerpoint (Microsoft Office Professional Plus 2016) computer software.

Serial sections and reconstruction

Immunoprocessed and post-fixed flat-embedded sections through the prPFC were mounted on EPON blocks and ultrathin 110 nm sections were collected serially on formvar/carbon coated single slot grids. Sections were collected at 110 nm, rather than 80 nm, to enable collection of a maximal depth (ie, throughout a synaptic terminal) on a minimal number of formvar/carbon grids while still allowing accurate visibility of synaptic specializations. Imaging commenced in the middle of a series of sections (typically ~20–25 sections) where a CB1-immunoreactive axon terminal was clearly visible. The same axon terminal was then identified in adjacent sections and imaged throughout its depth. Serial reconstruction was performed using Reconstruct computer software, downloaded from http://synapseweb.clm.utexas.edu/software-0, and funded in part from the National Institutes of Health and the Human Brain Project (P30 HD18655, R01 MH/DA 57351, and R01 EB 002170).

Results

Morphology of CB1-containing axon terminals

The CB1 receptor was chiefly contained within axon terminals of the prPFC and BLA, and was also infrequently observed within glia or soma. Axon terminals immunolabeled for the CB1 receptor that targeted neuronal soma often formed invaginated synapses in both the prPFC and BLA (Fig 1c–e), thereby increasing the surface area between the presynaptic terminal and cell body. These invaginated synapses were not observed within small or medium-sized dendrites. CB1-containing axon terminals also frequently contained dense-core vesicles (Fig 1d–f). CB1-containing axon terminals often were positioned opposite to folds of endomembranes in neuronal soma and dendrites (Fig 1g).

Some CB1-immunoreactive axon terminals were positioned between apposing neuronal somata in layer III of the prPFC (Fig 2a–b). These axon terminals were large and contacted both somata. These uniquely positioned axon terminals often formed inhibitory-type synapses with one or both somata, potentially facilitating somatic coordination via eCB release from one neuron to attenuate neurotransmitter release onto its neighbor.

Inhibitory and excitatory CB1-immunoreactive synapses

The CB1 receptor is primarily contained within inhibitory-type axon terminals of the prPFC and BLA. 2064 CB1-containing axon terminals were counted—1457 throughout all layers of the prPFC and 607 in the BLA. Within the prPFC, 242 CB1-containing terminals formed discernible synaptic specializations within the plane of section and in the BLA, 151 formed discernible synaptic specializations. CB1-containing axon terminals forming asymmetric excitatory-type synapses in the BLA or the prPFC were infrequent. These excitatory-type asymmetric terminals targeted dendritic spines (Fig 3a) or the dendritic shaft. The vast majority of synapses formed by CB1-containing axon terminals in both brain regions were symmetric inhibitory-type (Fig 3b) and contacted dendrites or somata. In the prPFC, 95% (230) of CB1-containing axon terminals were symmetric inhibitory-type while in the BLA, 90% (136) of axon terminals containing CB1 formed symmetric inhibitory-type junctions. CB1-containing axon terminals were not distributed significantly differently between asymmetric excitatory-type and symmetric inhibitory-type synaptic specializations in the BLA relative to the prPFC, although there is a statistical trend ($p < 0.1$) towards a greater probability of asymmetric CB1 synapses in the BLA than the prPFC (Chi-squared = 3.597, $p = 0.058$). CB1-containing axon terminals primarily contacted dendrites and neuronal somata in both the prPFC and the BLA.

Proximity of dendritic mGluR5 immunogold to CB1 axon terminals

The mGluR5 labeling was primarily located within somata, dendrites, and dendritic spines of the prPFC and BLA and was more rarely observed in glia, axons, and axon terminals. Within soma labeled for mGluR5, immunogold particles frequently localized to endomembranes, including the Golgi apparatus, and were also seen on the interior nuclear membrane, where mGluR5 is thought to mediate changes in calcium ion changes in the nucleoplasm (Sergin et al. 2017). Dendrites immunolabeled for mGluR5 were frequently contacted by CB1-containing axon terminals (Fig 4a–e). Interestingly, many mGluR5-labeled dendrites contacted by CB1-containing terminals were also receptive to unlabeled axon terminals that formed asymmetric excitatory-type synapses (Fig 4a–e). The mGluR5 immunolabeled dendritic profiles were also frequently observed without any visible CB1 input (Fig 4f–i).

Quantitative comparison of immunolabeling in BLA and prPFC showed regional similarities and differences in the proportion of dendritic and axonal profiles expressing mGluR5 (Fig 4j). In the BLA, 56% of mGluR5 immunogold-labeled profiles were dendrites, 21% dendritic spines, 6% axon terminals, 6% axons, 9% neuronal soma, less than 1% were glia and 2% were not definitively identifiable. In the prPFC, a similar distribution was observed: 72% of mGluR5-containing profiles were dendrites, 13% dendritic spines, 3% axon terminals, 4% axons, 6% neuronal soma, 2% glia, and 1% could not be identified.

To investigate the relationship between dendritic mGluR5 and synaptic input, we measured the distances between mGluR5 immunogold particles and axon terminals (1) forming excitatory-type synapses or (2) containing CB1-receptors whenever present in a single plane of section. Distance was measured from the dendritic immunogold particle to the nearest point of contact with the synaptic specialization. The distance between mGluR5 immunogold particles and asymmetric synapses was not significantly different from the distance between the immunogold particles and CB1-containing axon terminals (Fig 4k). To confirm that these statistically equivalent means were not due to a bimodal distribution of mGluR5 distance to either type of axon terminal, the percentage distribution of mGluR5 distance was binned by 0.1 nm increments. The mGluR5 immunogold distribution distance was thereby observed to be similar for glutamate or CB1 terminals (Fig 4l), possibly indicating a similarly strategic positioning of mGluR5 near either glutamatergic or CB1-containing axon terminals, as shown qualitatively in Fig 4a–i.

Inhibitory CB1-containing axon terminals and unlabeled excitatory-type axon terminals converge upon the same postsynaptic target

In the prPFC, 95% of all axon terminals with detectible CB1 immunoreactivity were GABAergic inhibitory-type. The mGluR5-containing dendrites contacted by CB1-labeled axon terminals also frequently receive input from unlabeled axon terminals forming asymmetric, excitatory-type synapses. Although both the symmetric and the asymmetric synaptic specializations were sometimes present in the same plane of section, the angle of sectioning could result in proximal synapses not being observed within the same section. This could result in an underestimation of the degree of convergence of inhibitory-type CB1-containing terminals and excitatory-type terminals on common dendrites when analyzing single planes of section. Therefore, to determine accurately whether a dendrite postsynaptic to a CB1-containing dendrite is also typically proximally receptive to excitatory-type inputs, analysis of sequential sections is required. Serial section analysis was undertaken on prPFC dendrites postsynaptic to CB1-containing terminals, following them throughout the span of contact with the CB1 terminal (Fig 5).

We analyzed 18 CB1-containing axon terminals using serial sectioning. Because of steric hindrances, immunogold particles cannot penetrate as robustly or as deeply into tissue as immunoperoxidase, and therefore mGluR5 was not quantified in serial section analysis.

Of the 18 CB1 axon terminals examined, 17 terminated on dendritic profiles and one targeted a neuronal soma. Three CB1-containing terminals formed *en passant* synapses. The single CB1 axon terminal targeting a neuronal soma had a depth exceeding the 2420 nm cumulative depth of the serial sections collected in that series. This is far larger than the CB1-labeled terminals terminating on dendritic shafts, which had a mean depth of 1100 ± 91 nm, and ranged from 440 nm-1650 nm.

It was not possible to discern a synaptic specialization in 3 of 18 terminals because the plane of sectioning was tangential to the synapse. The remaining 15 CB1-containing axon terminals formed symmetric inhibitory-type synaptic specializations. Of the 15 postsynaptic targets of GABAergic CB1 terminals, 13 were also contacted by proximal glutamatergic input (Fig 5a–c). The asymmetric postsynaptic density, the active zone of the glutamatergic

input, typically was observed within one or two serial sections of the active zone of the CB1 terminal (average z-axis distance = 141 ± 42 nm).

In the instance shown in Figure 5, the postsynaptic convergent target of the CB1/inhibitory type terminal and the excitatory-type terminal occurs at the point of dendritic bifurcation. This was a common motif: CB1-containing axon terminals targeted a point of dendritic bifurcation in 50% (9/18) of the synapses analyzed. The reconstruction of the serial sections in Fig 5a–h, showing a CB1-containing axon terminal, glutamatergic axon terminal, and convergent postsynaptic target, is illustrated in Fig 5i–j.

Discussion

Our results provide ultrastructural evidence that CB1 receptors in both the prPFC and BLA are primarily located in complex inhibitory-type axon terminals that converge with excitatory-type synapses on somatodendritic profiles expressing mGluR5, often at a dendritic branch point or between two neuronal somata. This synaptic arrangement suggests that endocannabinoid-regulated plasticity in cortical structures may often involve heterosynaptic mechanisms (Fig 6).

However, CB1 expression patterns change over postnatal and adolescent development (Cass DK et al. 2014) and CB1-influenced behaviors differ between males and females (Castelli MP et al. 2014). Thus, the presently described ultrastructural architecture of CB1 terminals in the prPFC of adult male rats may differ from that seen prior to the adolescent/adult transition, and in females.

Regional specificity of CB1 receptor expression

Within the prPFC and BLA, CB1 receptors are primarily localized to presynaptic terminals and axonal processes and was also infrequently observed in somata and glia (unpublished observations; see also Oliveira da Cruz et al. 2016 and Howlett and Abood 2017). This is consistent with past reports in the hippocampus (Katona et al. 1999), PFC (Fitzgerald et al. 2013), and the somatosensory cortex (Bodor *et al.* 2005). In the caudate putamen, however, the CB1 receptor is also abundantly detected in glial processes, dendrites, and dendritic spines (Rodriguez et al. 2001; Pickel et al. 2004). This evidence indicates that the cellular and subcellular targeting of CB1 receptors is specific and unique to different brain areas, and that CB1 receptor expression patterns are different in striatal relative to cortical and hippocampal brain regions. Furthermore, even though the CB1 receptor is principally detected in presynaptic axon terminals in both the prPFC and BLA, there is a trend towards an increased percentage of CB1-containing asymmetric excitatory axon terminals in the BLA relative to symmetric. This may indicate a subtle region-specific preferential targeting of the CB1 receptor to excitatory terminals in the BLA as compared to the prPFC. Activation of BLA CB1 receptors could therefore have an increased dampening effect on glutamatergic transmission (Azad et al. 2003).

CB1 receptors are expressed in complex inhibitory-type terminals in the prPFC and BLA

The vast majority of axon terminals containing detectible CB1 immunoreactivity formed symmetric, inhibitory-type synapses or were without discernible synaptic membrane

specializations in the plane of section. It is, however, possible that excitatory axon terminals of the prPFC and BLA contain CB1 receptors in too low abundance to produce detectible immunoreactivity throughout the terminal, leading to underestimation of excitatory CB1-containing axon terminals. This does not discount the potential importance of CB1 receptors expressed at low levels on excitatory type terminals, especially because these receptors may be more effective at inducing a G-protein coupled response than those on inhibitory axon terminals (Steindel et al. 2013).

CB1 immunoreactive axon terminals in the prPFC and BLA are shown to possess a diversity of synaptic vesicles and to form complex, invaginated synapses onto soma and proximal domains of dendrites. These are characteristic features of inhibitory interneurons in the cerebral cortex (Druga 2009), where GABAergic terminals are characterized by many small clear vesicles and symmetric membrane specializations comparable to those showing CB1 immunoreactivity in the PFC and BLA. Inhibitory CB1-containing axon terminals frequently target large pyramidal soma in the PFC (Hill et al. 2011) and the BLA (Vereczki et al. 2016), which are also targeted by a non-overlapping population of axon terminals from parvalbumin interneurons (Fitzgerald et al. 2012). Because activation of the CB1 receptor leads to dampening of GABA(A) mediated induced postsynaptic currents (Katona et al. 2001), the CB1 receptor is therefore well-placed to modulate the inhibition of pyramidal output from both the BLA and the PFC.

Many CB1-labeled terminals in our study also contained several large dense core vesicles that are known storage sites for cholecystokinin (CCK) and other neuropeptides found in many inhibitory interneurons in the cerebral cortex (Hill et al. 2007). This suggests that these neurons are the source of many of the CB1 labeled inhibitory terminals presynaptic to mGluR5 in these regions. These findings are in agreement with the expression of CB1 in a subpopulation of CCK-containing interneurons in the amygdala (McDonald and Mascagni 2001), and are also consistent with findings in the mouse forebrain (Marsicano and Lutz 1999).

Additionally, many CB1-containing axon terminals apposed swaths of endomembranes, supporting the hypothesis that lipid rafts may play a role in the uptake and recycling of endocannabinoids (McFarland and Barker 2004). Omiya et al (Omiya et al. 2015) showed comparable complex axon terminals formed by VGluT3-expressing CCK-positive basket cells in the amygdala and cortex, some of which juxtaposed clusters of endocannabinoid synthesizing enzyme diacylglycerol lipase-α immunoreactivity. Our findings confirm that CB1-containing axon terminals in these same brain regions, many of which appose mGluR5, form the same type of synaptic structure, which might be important for the recruitment and stabilization of endocannabinoid-synthesizing molecules.

CB1-containing axon terminals target specialized somatodendritic locations

Axon terminals immunoreactive for CB1 receptors in the prPFC and BLA often terminated on somata and large dendrites that are known to be particularly strong regulators of synaptic strength (de Jong et al. 2012). CB1 receptor labeling was also seen in terminals having other distinct morphological targets, such as at the point of dendritic bifurcation, or between two neuronal somata. Branch points of the apical dendritic tree of pyramidal neurons are

uniquely sensitive regions in the regulation of dendritic excitability (Ferrante et al. 2013). By preferentially targeting dendritic bifurcations, CB1-containing axon terminals are positioned to mediate the synchronicity of synaptic input and dendritic branch excitability. Interestingly, mice lacking the CB1 receptor specifically in GABAergic neurons show decreased dendritic branching of pyramidal neurons in the hippocampus (Monory et al. 2015). Within the prPFC as well as the motor cortex, mice lacking the CB1 receptor have reduced dendritic branching (Ballesteros-Yanez et al. 2007; Hill, Hillard, et al. 2011). These observations, combined with the preferential targeting of dendritic branch points by CB1 axon terminals revealed by serial sectioning, indicates that the CB1 receptor plays a crucial role in the development of pyramidal neuron structure and an ongoing role in regulating pyramidal neuron signaling.

Inhibitory-type CB1 terminals converge with excitatory-type terminals on somatodendritic profiles expressing mGluR

The postsynaptic targets of CB1 axon terminals throughout the prPFC and the BLA were neuronal soma and dendrites, many of which contained mGluR5. These mGluR5 dendrites were also targeted by unlabeled axon terminals apposing asymmetric postsynaptic specializations typical of indicative of glutamatergic terminals input. Serial section analysis of the prPFC revealed that CB1-containing inhibitory-type terminals usually contacted dendrites that were also receptive to local glutamatergic input. These results provide the first ultrastructural evidence for a mechanism of heterosynaptic plasticity whereby glutamatergic mGluR5 activation can drive CB1-mediated suppression of synaptic vesicle release from GABAergic axon terminals in the PFC.

This data is supported by electrophysiological research in the hippocampus (Varma et al. 2001), where glutamate release by Schaffer collaterals activates mGluR1/5 on dendrites of CA1 pyramidal neurons. This induces a lasting inhibition of GABA release from neighboring axon terminals that is dependent upon eCBs (Chevaleyre and Castillo 2003). A similar mechanism induces mGluR5-mediated retrograde suppression of GABA release via eCB/CB1 signaling in a cell preparation from the BLA which consisted of a postsynaptic neuron and attached synaptic boutons (Zhu and Lovinger 2005). This allows for cannabinoid-mediated regulation of long-term potentiation to be targeted to specific synapses, as described in the rat hippocampus (Carlson et al. 2002). In the PFC, mGluR5 activation in concert with CB1-mediated suppression of inhibition induced increased output of pyramidal neurons (Kiritoshi *et al.* 2013).

Group 1 mGluRs have been shown to amplify glutamate signaling through the ionotropic glutamate NMDA receptor (Fitzjohn et al. 1996), affecting long-term neuronal patterning, excitatory signaling, and synapse selectivity (Kotecha *et al.* 2003; Wijetunge et al. 2008; Chen et al. 2012). The ultrastructural evidence described in our study suggests an additional plausible mechanism for mGluR5-mediated upregulation of excitatory output: through CB1-mediated depression of key local GABAergic synapses.

Implications

The results of this study hold potentially important implications for treating diverse disorders characterized in part by PFC dysfunction. Schizophrenia, for instance, manifests near the adolescent/adult transition, a developmental timepoint coincident with decreasing PFC CB1 expression (Heng et al. 2011). Positive allosteric modulators of mGluR5 increase cognitive function and have shown promise as potential antipsychotics in animal models of schizophrenia (Vinson and Conn 2012). Chronic pain is likewise characterized in part by abnormal inhibition of PFC pyramidal neuron output to the amygdala (Ji et al. 2010), which can be ameliorated through a combination of an mGluR5 positive allosteric modulator and CB1 agonist (Ji and Neugebauer 2014).

The function of allosteric modulators of mGluR5 is facilitated by coactivation of the CB1 receptor (Kiritoshi *et al.* 2013; Ji and Neugebauer 2014). Our work illuminates the ultrastructural architecture that underlies increased pyramidal output from the PFC after administration of a positive allosteric modulator of mGluR5 (Kiritoshi *et al.* 2013; Ji and Neugebauer 2014), and furthermore supports a mechanism by which endocannabinoid signaling can fine-tune PFC pyramidal neuron output.

Acknowledgements

This work was supported by the National Institute on Drug Abuse (grant numbers T32DA7274 to MLF; NIDA DA021696 to KM; and DA042943 to VMP) and the National Institute of Mental Health (grant number T32MH15144 to MLF).

References

Azad SC, Eder M, Marsicano G, Lutz B, Zieglgansberger W, Rammes G. 2003 Activation of the cannabinoid receptor type 1 decreases glutamatergic and GABAergic synaptic transmission in the lateral amygdala of the mouse. Learn Mem. 10:116–128. [PubMed: 12663750]

Ballesteros-Yanez I, Valverde O, Ledent C, Maldonado R, DeFelipe J. 2007 Chronic cocaine treatment alters dendritic arborization in the adult motor cortex through a CB1 cannabinoid receptor-dependent mechanism. Neuroscience. 146:1536–1545. [PubMed: 17467187]

Berghuis P, Rajnicek AM, Morozov YM, Ross RA, Mulder J, Urban GM, Monory K, Marsicano G, Matteoli M, Canty A, Irving AJ, Katona I, Yanagawa Y, Rakic P, Lutz B, Mackie K, Harkany T. 2007 Hardwiring the brain: endocannabinoids shape neuronal connectivity. Science. 316:1212–1216. [PubMed: 17525344]

Bodor AL, Katona I, Nyiri G, Mackie K, Ledent C, Hajos N, Freund TF. 2005 Endocannabinoid signaling in rat somatosensory cortex: laminar differences and involvement of specific interneuron types. The Journal of neuroscience : the official journal of the Society for Neuroscience. 25:6845–6856. [PubMed: 16033894]

Carlson G, Wang Y, Alger BE. 2002 Endocannabinoids facilitate the induction of LTP in the hippocampus. Nature neuroscience. 5:723–724. [PubMed: 12080342]

Chen CC, Lu HC, Brumberg JC. 2012 mGluR5 knockout mice display increased dendritic spine densities. Neuroscience letters. 524:65–68. [PubMed: 22819970]

Chevaleyre V, Castillo PE. 2003 Heterosynaptic LTD of hippocampal GABAergic synapses: a novel role of endocannabinoids in regulating excitability. Neuron. 38:461–472. [PubMed: 12741992]

de Jong AP, Schmitz SK, Toonen RF, Verhage M. 2012 Dendritic position is a major determinant of presynaptic strength. The Journal of cell biology. 197:327–337. [PubMed: 22492722]

Devane WA, Hanus L, Breuer A, Pertwee RG, Stevenson LA, Griffin G, Gibson D, Mandelbaum A, Etinger A, Mechoulam R. 1992 Isolation and structure of a brain constituent that binds to the cannabinoid receptor. Science. 258:1946–1949. [PubMed: 1470919]

Druga R 2009 Neocortical inhibitory system. Folia biologica. 55:201–217. [PubMed: 20163769]

Ferrante M, Migliore M, Ascoli GA. 2013 Functional impact of dendritic branch-point morphology. The Journal of neuroscience : the official journal of the Society for Neuroscience. 33:2156–2165. [PubMed: 23365251]

Fitzgerald ML, Chan J, Mackie K, Lupica CR, Pickel VM. 2012 Altered dendritic distribution of dopamine D2 receptors and reduction in mitochondrial number in parvalbumin-containing interneurons in the medial prefrontal cortex of cannabinoid-1 (CB1) receptor knockout mice. The Journal of comparative neurology. 520:4013–4031. [PubMed: 22592925]

Fitzgerald ML, Mackie K, Pickel VM. 2013 The impact of adolescent social isolation on dopamine D2 and cannabinoid CB1 receptors in the adult rat prefrontal cortex. Neuroscience. 235:40–50. [PubMed: 23333674]

Fitzjohn SM, Irving AJ, Palmer MJ, Harvey J, Lodge D, Collingridge GL. 1996 Activation of group I mGluRs potentiates NMDA responses in rat hippocampal slices. Neuroscience letters. 203:211–213. [PubMed: 8742030]

Heng L, Beverley JA, Steiner H, Tseng KY. 2011 Differential developmental trajectories for CB1 cannabinoid receptor expression in limbic/associative and sensorimotor cortical areas. Synapse. 65:278–286. [PubMed: 20687106]

Herkenham M, Lynn AB, Johnson MR, Melvin LS, de Costa BR, Rice KC. 1991 Characterization and localization of cannabinoid receptors in rat brain: a quantitative in vitro autoradiographic study. The Journal of neuroscience : the official journal of the Society for Neuroscience. 11:563–583. [PubMed: 1992016]

Hill EL, Gallopin T, Ferezou I, Cauli B, Rossier J, Schweitzer P, Lambolez B. 2007 Functional CB1 receptors are broadly expressed in neocortical GABAergic and glutamatergic neurons. Journal of neurophysiology. 97:2580–2589. [PubMed: 17267760]

Hill MN, Hillard CJ, McEwen BS. 2011 Alterations in corticolimbic dendritic morphology and emotional behavior in cannabinoid CB1 receptor-deficient mice parallel the effects of chronic stress. Cereb Cortex. 21:2056–2064. [PubMed: 21263035]

Hill MN, McLaughlin RJ, Pan B, Fitzgerald ML, Roberts CJ, Lee TT, Karatsoreos IN, Mackie K, Viau V, Pickel VM, McEwen BS, Liu QS, Gorzalka BB, Hillard CJ. 2011 Recruitment of prefrontal cortical endocannabinoid signaling by glucocorticoids contributes to termination of the stress response. The Journal of neuroscience : the official journal of the Society for Neuroscience. 31:10506–10515. [PubMed: 21775596]

Howlett AC, Abood ME. 2017 CB1 and CB2 Receptor Pharmacology. Adv Pharmacol. 80:169–206. [PubMed: 28826534]

Ji G, Neugebauer V. 2014 CB1 augments mGluR5 function in medial prefrontal cortical neurons to inhibit amygdala hyperactivity in an arthritis pain model. The European journal of neuroscience. 39:455–466. [PubMed: 24494685]

Ji G, Sun H, Fu Y, Li Z, Pais-Vieira M, Galhardo V, Neugebauer V. 2010 Cognitive impairment in pain through amygdala-driven prefrontal cortical deactivation. The Journal of neuroscience : the official journal of the Society for Neuroscience. 30:5451–5464. [PubMed: 20392966]

Katona I, Rancz EA, Acsady L, Ledent C, Mackie K, Hajos N, Freund TF. 1999 Distribution of CB1 cannabinoid receptors in the amygdala and their role in the control of GABAergic transmission. The Journal of neuroscience : the official journal of the Society for Neuroscience. 19:4544–4558. [PubMed: 10341254]

Katona I, Urban GM, Wallace M, Ledent C, Jung KM, Piomelli D, Mackie K, Freund TF. 2006 Molecular composition of the endocannabinoid system at glutamatergic synapses. The Journal of neuroscience : the official journal of the Society for Neuroscience. 26:5628–5637. [PubMed: 16723519]

Kiritoshi T, Sun H, Ren W, Stauffer SR, Lindsley CW, Conn PJ, Neugebauer V. 2013 Modulation of pyramidal cell output in the medial prefrontal cortex by mGluR5 interacting with CB1. Neuropharmacology. 66:170–178. [PubMed: 22521499]

Kotecha SA, Jackson MF, Al-Mahrouki A, Roder JC, Orser BA, MacDonald JF. 2003 Co-stimulation of mGluR5 and N-methyl-D-aspartate receptors is required for potentiation of excitatory synaptic

transmission in hippocampal neurons. The Journal of biological chemistry. 278:27742–27749. [PubMed: 12740378]

Kuwajima M, Hall RA, Aiba A, Smith Y. 2004 Subcellular and subsynaptic localization of group I metabotropic glutamate receptors in the monkey subthalamic nucleus. The Journal of comparative neurology. 474:589–602. [PubMed: 15174075]

Lafourcade M, Elezgarai I, Mato S, Bakiri Y, Grandes P, Manzoni OJ. 2007 Molecular components and functions of the endocannabinoid system in mouse prefrontal cortex. PloS one. 2:e709. [PubMed: 17684555]

Lane DA, Chan J, Fitzgerald ML, Kearn CS, Mackie K, Pickel VM. 2012 Quinpirole elicits differential in vivo changes in the pre- and postsynaptic distributions of dopamine D(2) receptors in mouse striatum: relation to cannabinoid-1 (CB(1)) receptor targeting. Psychopharmacology. 221:101–113. [PubMed: 22160162]

Lovinger DM. 2008 Presynaptic modulation by endocannabinoids. Handbook of experimental pharmacology.435–477. [PubMed: 18064422]

Maejima T, Hashimoto K, Yoshida T, Aiba A, Kano M. 2001 Presynaptic inhibition caused by retrograde signal from metabotropic glutamate to cannabinoid receptors. Neuron. 31:463–475. [PubMed: 11516402]

Marsicano G, Lutz B. 1999 Expression of the cannabinoid receptor CB1 in distinct neuronal subpopulations in the adult mouse forebrain. The European journal of neuroscience. 11:4213–4225. [PubMed: 10594647]

McDonald AJ, Mascagni F. 2001 Localization of the CB1 type cannabinoid receptor in the rat basolateral amygdala: high concentrations in a subpopulation of cholecystokinin-containing interneurons. 107:641–52.

McFarland MJ, Barker EL. 2004 Anandamide transport. Pharmacology & therapeutics. 104:117–135. [PubMed: 15518883]

Monory K, Polack M, Remus A, Lutz B, Korte M. 2015 Cannabinoid CB1 receptor calibrates excitatory synaptic balance in the mouse hippocampus. The Journal of neuroscience : the official journal of the Society for Neuroscience. 35:3842–3850. [PubMed: 25740514]

Oliveira da Cruz JF, Robin LM, Drago F, Marsicano G, Metna-Laurent M. 2016 Astroglial type-1 cannabinoid receptor (CB1): A new player in the tripartite synapse. Neuroscience. 323:35–42. [PubMed: 25967266]

Omiya Y, Uchigashima M, Konno K, Yamasaki M, Miyazaki T, Yoshida T, Kusumi I, Watanabe M. 2015 VGluT3-expressing CCK-positive basket cells construct invaginating synapses enriched with endocannabinoid signaling proteins in particular cortical and cortex-like amygdaloid regions of mouse brains. The Journal of neuroscience : the official journal of the Society for Neuroscience. 35:4215–4228. [PubMed: 25762668]

Pickel VM, Chan J, Kash TL, Rodriguez JJ, MacKie K. 2004 Compartment-specific localization of cannabinoid 1 (CB1) and mu-opioid receptors in rat nucleus accumbens. Neuroscience. 127:101–112. [PubMed: 15219673]

Rodriguez JJ, Mackie K, Pickel VM. 2001 Ultrastructural localization of the CB1 cannabinoid receptor in mu-opioid receptor patches of the rat Caudate putamen nucleus. The Journal of neuroscience : the official journal of the Society for Neuroscience. 21:823–833. [PubMed: 11157068]

Sergin I, Jong YI, Harmon SK, Kumar V, O'Malley K. 2017 Sequences within the C-terminus of the metabotropic glutamate receptor, mGluR5, are responsible for inner nuclear localization. The Journal of Biological Chemistry. 292, 3637–3655. [PubMed: 28096465]

Steindel F, Lerner R, Haring M, Ruehle S, Marsicano G, Lutz B, Monory K. 2013 Neuron-type specific cannabinoid-mediated G protein signalling in mouse hippocampus. Journal of neurochemistry. 124:795–807. [PubMed: 23289830]

Stella N, Schweitzer P, Piomelli D. 1997 A second endogenous cannabinoid that modulates long-term potentiation. Nature. 388:773–778. [PubMed: 9285589]

Trivedi RR, Bhattacharyya S. 2012 Constitutive internalization and recycling of metabotropic glutamate receptor 5 (mGluR5). Biochemical and biophysical research communications. 427:185–190. [PubMed: 22995293]

Varma N, Carlson GC, Ledent C, Alger BE. 2001 Metabotropic glutamate receptors drive the endocannabinoid system in hippocampus. The Journal of neuroscience : the official journal of the Society for Neuroscience. 21:RC188. [PubMed: 11734603]

Vereczki VK, Veres JM, Muller K, Nagy GA, Racz B, Barsy B, Hajos N. 2016 Synaptic organization of perisomatic GABAergic inputs onto the principal cells of the mouse basolateral amygdala. Frontiers in neuroanatomy. 10:20. [PubMed: 27013983]

Vinson PN, Conn PJ. 2012 Metabotropic glutamate receptors as therapeutic targets for schizophrenia. Neuropharmacology. 62:1461–1472. [PubMed: 21620876]

Wijetunge LS, Till SM, Gillingwater TH, Ingham CA, Kind PC. 2008 mGluR5 regulates glutamate-dependent development of the mouse somatosensory cortex. The Journal of neuroscience : the official journal of the Society for Neuroscience. 28:13028–13037. [PubMed: 19052194]

Wilson RI, Nicoll RA. 2001 Endogenous cannabinoids mediate retrograde signalling at hippocampal synapses. Nature. 410:588–592. [PubMed: 11279497]

Zhu PJ, Lovinger DM. 2005 Retrograde endocannabinoid signaling in a postsynaptic neuron/synaptic bouton preparation from basolateral amygdala. The Journal of neuroscience : the official journal of the Society for Neuroscience. 25:6199–6207. [PubMed: 15987949]

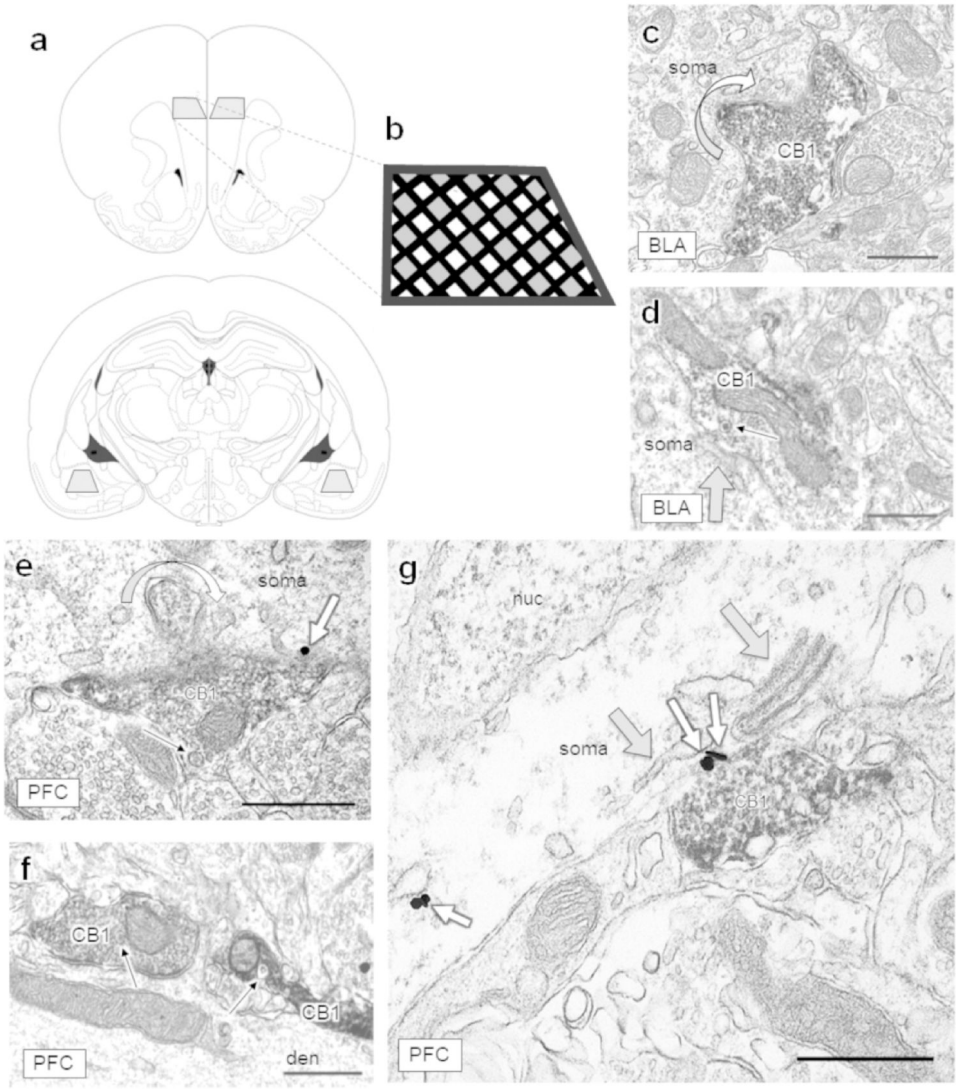

Figure 1: Neuronal regions selected for single-section analysis and morphological features of CB1-containing axon terminals.

(a) Grey trapezoids represent the regions examined. The prelimbic region of the PFC (top) and the basolateral region of the amygdala (bottom) were sampled bilaterally. *Images adapted from Paxinos and Watson, 1997.* (b) Black lines represent the grid bars of the copper grid and grey shaded regions represent areas where micrographs were typically captured. The PFC was sampled throughout layers II-V/VI. CB1 immunoreactive axon terminals were very rarely present in layer I but were abundant throughout all other layers. (c-d) CB1-containing axon terminals contact neuronal somata in the BLA and (e-g) somata and large dendrites in the PFC. (c) A curved arrow shows a CB1-containing axon terminal protruding into a neuronal soma in the BLA and (e) in the PFC, creating increased surface area between CB1-containing terminals and postsynaptic targets, which sometimes contained mGluR5 immunogold (small white arrows). Dense core vesicles (narrow black arrows) are often visible within CB1 axon terminals of the BLA (d) and PFC (e-f). (g) Folds of endomembranes (grey arrows; also in d) were often observed adjacent to CB1-containing

terminals. CB1 = CB1-containing axon terminal, den = dendrite, nuc = nucleus. Scale bars = 500 nm.

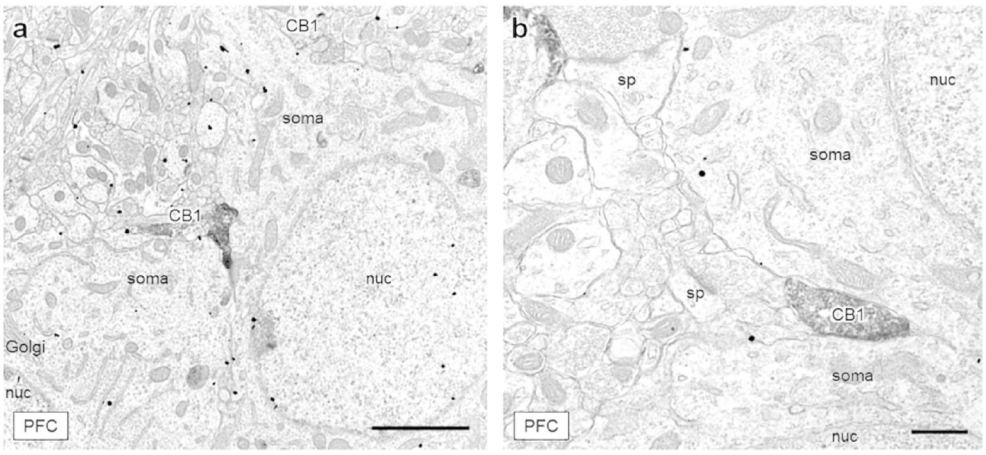

Figure 2: CB1-containing axon terminals positioned between two neuronal soma.

(a) A large CB1-labeled axon terminal (CB1) is sandwiched between two mGluR5-labeled soma in layer III of the mPFC. Another lightly labeled, irregularly shaped CB1-containing terminal contacts the upper soma at a point of dendritic branching. (b) An axon terminal containing CB1 immunoreactivity is positioned between two tightly apposed neuronal soma, also in layer III of the mPFC. Scale bar (a) = 2 μm, scale bar (b) = 500 nm, CB1 = CB1-containing axon terminal, Golgi = Golgi apparatus, nuc = nucleus, sp = dendritic spine.

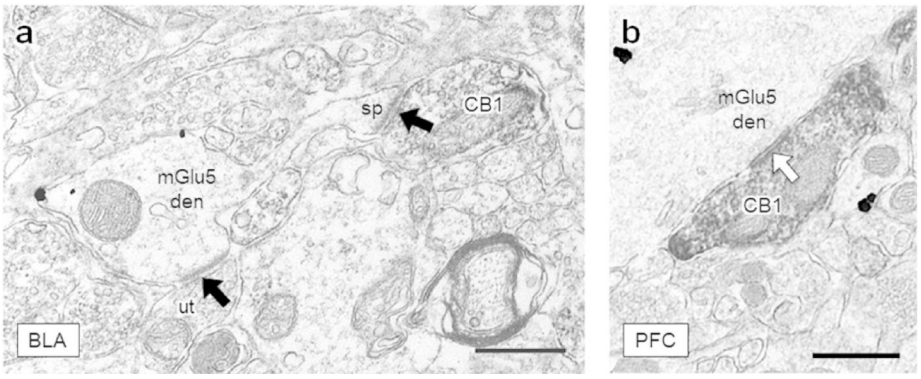

Figure 3: CB1-containing axon terminals form synapses in the BLA and PFC.

(a) A CB1-labeled axon terminal forms an asymmetric excitatory-type synapse (black arrow) with a spine protruding from a nearby mGlu5-containing dendrite in the BLA. An unlabeled terminal (ut) forms an excitatory synapse onto the dendritic shaft. (b) An axon terminal containing CB1 immunoreactivity forms a symmetric inhibitory-type specialization (white arrow) with a large dendrite. Scale bars = 500 nm, CB1 = CB1-containing terminal, mGlu5 den = dendrite containing mGlu5 immunogold, ut = unlabeled terminal, sp = dendritic spine.

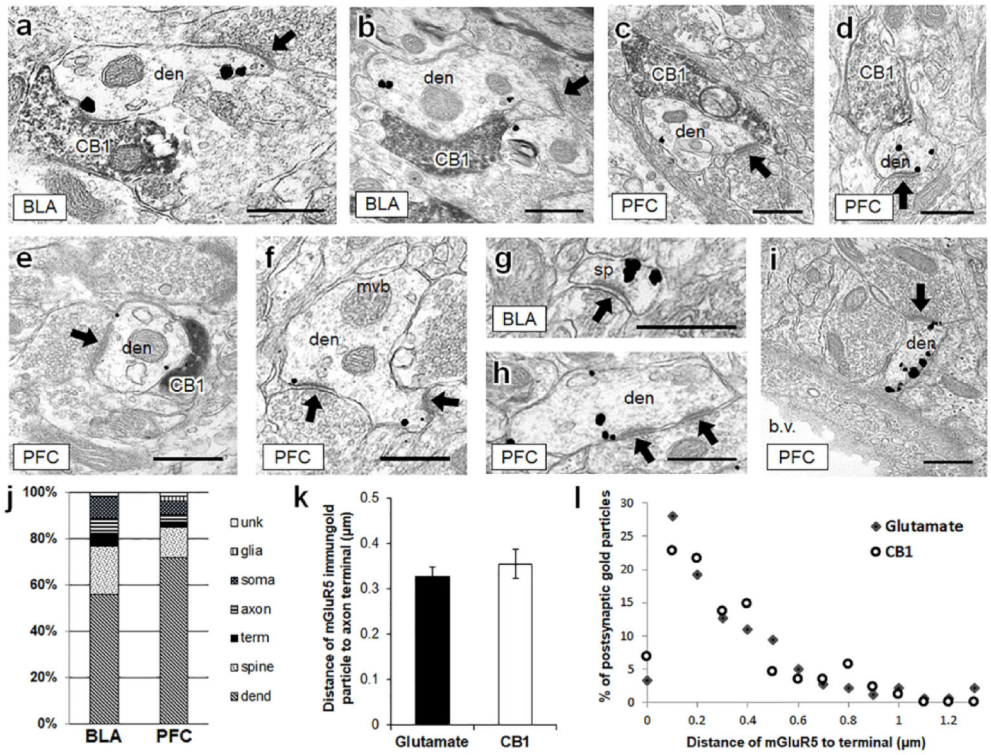

Figure 4: In the BLA and PFC, mGluR5 immunogold is frequently contained within dendrites that are targeted by both CB1-containing axon terminals and glutamatergic axon terminals.

(a, b), In the BLA, dendrites containing punctate mGluR5 immunogold labeling are frequently contacted by CB1-containing axon terminals. These same dendrites also frequently form asymmetric excitatory-type postsynaptic densities with unlabeled terminals (black arrows). (c-e) The same synaptic motif is evident in mGluR5-containing dendrites of the PFC. (f-i) mGluR5 immunogold is also often seen in dendrites and dendritic spines without visible CB1 input. CB1 = CB1-containing axon terminal, den = mGluR5 dendrite, mvb = multi-vesicular body, sp = dendritic spine, b.v. = blood vessel. Scale bars = 500 nm. (j) In 865 mGluR5 labeled profiles counted in the BLA and PFC, mGluR5 immunogold was most frequently contained within dendrites and dendritic spines. (k) The distance of mGluR5 immunogold particles from glutamatergic and CB1-containing axon terminals is not significantly different in the PFC. (l) The distribution of mGluR5 immunogold particle distance from unlabeled glutamatergic terminals and CB1-containing terminals was binned by 0.1 µm increments. The distance between postsynaptic mGluR5 immunogold and CB1-containing or glutamate terminals follows a similar pattern. Unk = unidentifiable (unknown) profile, term = axon terminal, dend = dendrite.

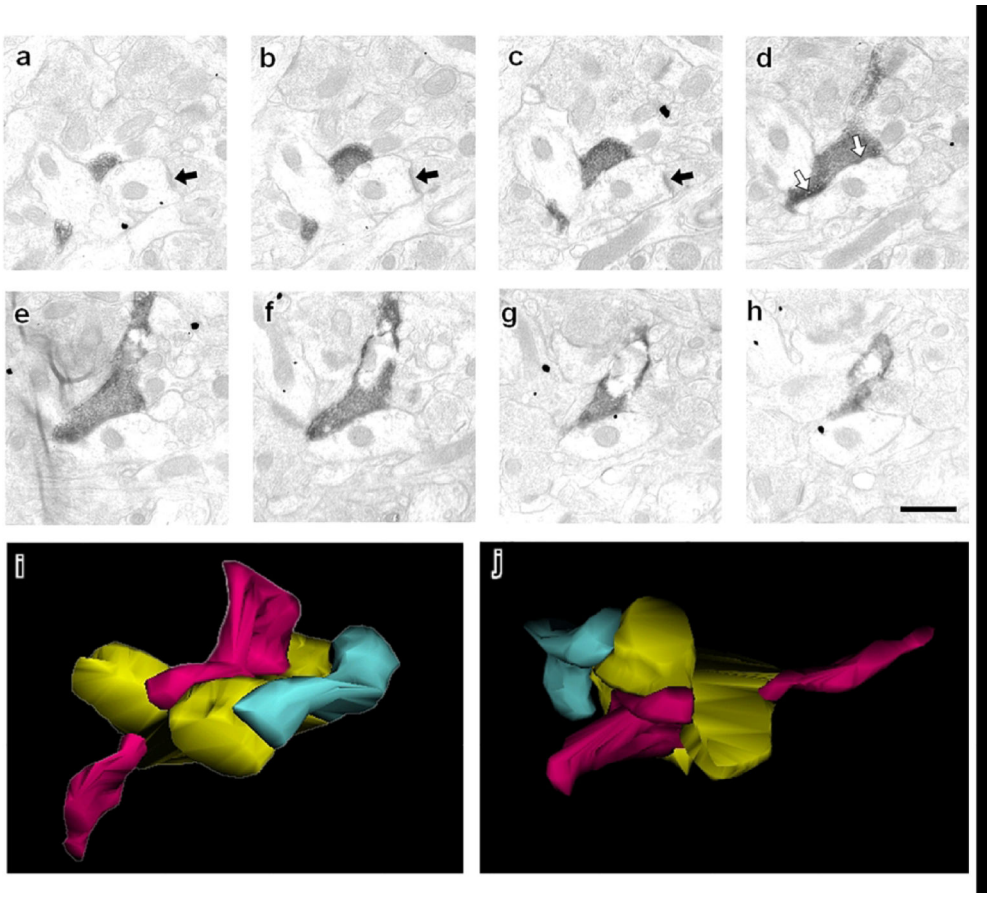

Figure 5: Serial sections follow a CB1-containing terminal in the mPFC through multiple planes of section.

(a-c) An asymmetric postsynaptic density indicative of an excitatory synapse (black arrow) is evident in a dendritic profile. (d) The same dendritic profile is targeted by an axon terminal containing CB1 immunoreactivity that forms symmetric inhibitory-type synapses (white arrows). This concurrence of glutamatergic and GABAergic input occurs at the point of a dendritic bifurcation. This is illustrated by (i-j) a serial reconstruction of this CB1 terminal. The CB1 axon terminal (magenta) targets a postsynaptic dendrite (gold) that is also contacted by a glutamatergic axon terminal (green). Two different views of the same three neuronal profiles are shown in i and j. Of the CB1 axon terminals that formed discernible synaptic specializations and were analyzed by serial section, 12 of 15 formed symmetric synapses on dendrites that were also receptive to glutamatergic input.

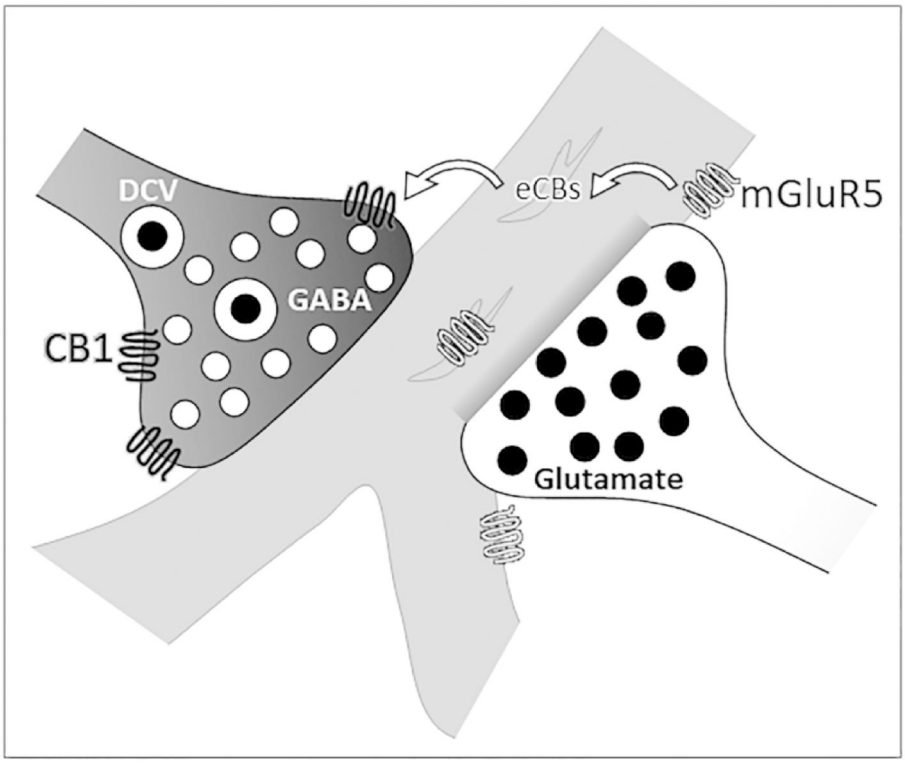

Figure 6: Schematic representation of CB1 and mGluR5 immunolabeling.

An axon terminal (white, on right) containing an excitatory neurotransmitter, illustrated here as glutamate, forms an asymmetric synapse on a dendritic shaft (gray) near a dendritic bifurcation. Glutamate released from this axon terminal is the ligand for mGluR5 on plasmalemmal and endomembranes of the postsynaptic dendrite. Activation of mGluR5 induces synthesis and release of endocannabinoids (eCBs). These eCBs may then bind presynaptic CB1 receptors on a different, inhibitory-type axon terminal (black, on left). Activation of the CB1 receptor leads to decreased release of dense-core (DCV) and small clear vesicles (illustrated here as GABA) from this terminal. In this way, glutamate signaling through the mGluR5 receptor can potentially attenuate the inhibitory input from a different axon terminal in a form of heterosynaptic plasticity.

Table 1:

Primary antisera used in experiments.

Primary antibody	Species raised in	Manufacturer	RRID	Dilution
CB1 receptor C terminus	Guinea pig, polyclonal			1:2000
mGlu5 receptor C terminus	Rabbit, polyclonal	Chemicon AB5675	AB_2295173	1:1000